

Effect of Nonequilibrium Charge Screening in $A + B \rightarrow 0$ Bimolecular Reactions in Condensed Matter

V. Kuzovkov¹ and E. Kotomin¹

Received May 6, 1992; final February 2, 1993

The formalism of many-particle densities developed earlier by the present authors is applied to the study of the cooperative effects in the kinetics of bimolecular $A + B \rightarrow 0$ reactions between oppositely charged particles (reactants). It is shown that unlike the Debye-Hückel theory in statistical physics, here charge screening has essentially a nonequilibrium character. For the asymmetric mobility of reactants ($D_A = 0$, $D_B \neq 0$) the joint spatial distribution of similar immobile reactants A reveals at short distances a singular character associated with their aggregation. The relevant reaction rate does not approach a steady state (as it does in the symmetric case, $D_A = D_B$), but increases infinitely in time, thus leading to a concentration decay which is quicker than the algebraic law generally accepted in chemical kinetics, $n \propto t^{-1}$.

KEY WORDS: Diffusion-limited reactions; charge screening; many-particle effects; self-organization; spatial correlations; Coulomb interaction.

1. INTRODUCTION

The kinetics of the $A + B \rightarrow 0$ bimolecular reaction between charged particles (reactants) is treated traditionally in terms of the *law of mass action*.⁽¹⁾ Assuming that $n(t) = n_A(t) = n_B(t)$ and $e = e_A = -e_B$ (n and e are particle concentration and charge), one gets

$$\frac{dn(t)}{dt} = -K(t) n^2(t) \quad (1)$$

¹ Department of Theoretical Physics, University of Latvia, 19 Rainis, Riga, Latvia.

In the transient period the reaction rate $K(t)$ depends on the initial particle distribution, but as $t \rightarrow \infty$, it reaches the steady-state limit

$$K(\infty) = K_0 = 4\pi DR_{\text{eff}} \quad (2)$$

where $D = D_A + D_B$ is the sum of diffusion coefficients and R_{eff} is the effective reaction radius. In terms of the *black sphere* approximation (when AB pairs approaching to within certain critical distance r_0 instantly recombine) this radius is⁽²⁾

$$R_{\text{eff}} = r_0 \frac{L}{1 - \exp(-L)} \quad (3)$$

where the dimensionless parameter $L = R/r_0$ contains the so-called *Onsager radius*, which is defined through

$$R = \frac{e^2}{\epsilon k_B T} \quad (4)$$

The Onsager radius is the critical distance at which the energy of Coulomb interaction between particles equals the thermal energy, $k_B T$, and thus the particles are very likely to recombine.

The value of the parameter L entering Eq. (3) defines whether Coulomb attraction or recombination is predominant: as $L \ll 1$, $R_{\text{eff}} \approx r_0$, whereas in the opposite case $L \gg 1$, $R_{\text{eff}} \approx R$ (the effective recombination sphere equals the Onsager radius).

Despite the fact that Eqs. (2)–(4) have been widely and successfully used in interpreting actual experimental data,⁽¹⁾ they are not well justified theoretically: in fact, in their derivation the solution of a *pair* problem with *nonscreened potential* $U_{AB}(r) = -e^2/\epsilon r$ is used. However, in the statistical physics of a system of charged particles the so-called *Coulomb catastrophes*⁽³⁾ have been known for a long time and they arise just because of the neglect of the essentially *many-particle* charge screening.

An attempt⁽⁴⁾ to use the screened Coulomb interaction characterized by the phenomenological parameter, the Debye radius R_D ,⁽³⁾ does not solve the problem, since $K(\infty)$ has been still traditionally calculated in the same pair approximation.

Another important many-particle aspect of the bimolecular reaction kinetics was discovered recently for *neutral* particles, when $L = 0$.⁽⁵⁻⁹⁾ Both analytical calculations and computer simulations have demonstrated the unusual *asymptotic* decay law $n(t) \propto t^{-d/4}$ as $t \rightarrow \infty$ (d is the space dimension). The reaction rate is *reduced* here as compared with the standard chemical kinetics, $n(t) \propto t^{-1}$, because of nonequilibrium *pattern*

formation—in the course of reaction its volume is divided into domains with the distinctive size $\xi(t) = (Dt)^{1/2}$ (called also the *diffusion length*); each domain contains predominantly particles A or B only. In other words, the *statistical aggregation* of similar particles occurs and increases in time since local inhomogeneities in particle densities (unavoidably present in any random distribution) turn out to be more stable than an absolutely homogeneous (well-stirred) system of particles. This effect is known to be more pronounced for high initial particle concentrations and/or long reaction times.⁽⁷⁾

As was noted in ref. 5, for charged particles such a reduction of the reaction rate is unlikely to occur, since spatial fluctuations in particle densities are now governed not by $\xi(t)$, but the screening radius; Coulomb repulsion of similar particles prevents their aggregation.

As was demonstrated for the first time by us,⁽¹⁰⁾ charge screening in the bimolecular reaction is of a nonequilibrium character and is not determined uniquely by particle densities, as is known to be in an *equilibrium* system of charged particles. Indeed, diffusion (spatial particle motion) determining the reaction kinetics is quite slow. On the other hand, unlike equilibrium systems, now oppositely charged particles recombine. Let us represent the effective force of Coulomb attraction by $F = -e^2S/er^2$, where $S = S(r, t)$ is the *screening factor*. In the thermodynamic equilibrium state $S = S(r)$ only and is characterized by a single parameter R_D , besides $\lim_{r \rightarrow \infty} S(r) = 0$. For nonequilibrium screening $S_0(t) = \lim_{r \rightarrow \infty} S(r, t)$, which generally speaking is nonzero. It is shown⁽¹⁰⁾ that in the case of equal diffusion coefficients, $D_A = D_B$, $\lim_{t \rightarrow \infty} S_0(t) = 0$, i.e., the *quasi-equilibrium* charge distribution is formed at long reaction times. In other words, Eqs. (2)–(4) remain valid, but in the framework of the many-particle formalism⁽¹⁰⁾ there is a *dynamic interplay* between the reaction rate acceleration due to Coulomb repulsion of similar particles and the cutoff of their interaction caused by a screening.

However, there is an important case neglected in ref. 10 when charge screening could be *principally nonequilibrium* and thus Eqs. (2)–(4) are no longer valid. To demonstrate it, we assume that particles of one kind, say A, are immobile ($D_A = 0$). This situation was considered earlier in ref. 7 for *neutral* particles and a strong statistical aggregation of immobile particles was found to occur. This aggregation is not destroyed by the diffusive motion of reactants and leads to an additional reaction rate reduction, which was confirmed by computer simulations.⁽¹¹⁾ We show below that for the *charged particles* in question an aggregation also takes place, but has other consequences.

At long distances from the A-rich aggregate existing on the background of the uniform B distribution it resembles a superparticle with the

effective charge $e_{\text{eff}} \approx N_A e_A$, where N_A is the number of similar particles in the aggregate. As $L > 1$, the effective recombination radius is proportional to the product of charges [see Eq. (4)], i.e., $R_{\text{eff}} \approx N_A R$. For the qualitative estimate we take into account that diffusive motion of **B** destroys **A** aggregates, so that at the moment t the reaction kinetics is determined by the interaction between the aggregate **A** occupying the distinctive volume $V \approx \xi^3(t)$ and the background of **B**. As the upper limit estimate of N_A let us take the mean number of particles **A** in the volume V , $N_A = n(t) \xi^3(t)$. Substituting now the reaction rate $K(t) \approx 4\pi DRN_A$ into Eq. (1), one arrives at the new asymptotic law $n(t) \propto t^{-5/4}$, indicating that the reaction now is *accelerated*.

After these preliminary comments, Section 2 deals with the exact statement of the problem. Some results are presented in Section 3 and the conclusion is drawn in Section 4. Note that this problem applies to several fields of the chemical physics of condensed matter. In particular, it is true for radiation physics of ionic crystals,^(12,13) where primary Frenkel defects-vacancies are immobile below room temperature, whereas interstitial ions become mobile above typically 30 K; these defects are oppositely charged and interact via the Coulomb law.

2. KINETIC EQUATIONS

A set of the integrodifferential kinetic equations used below was derived and analyzed in ref. 10. We stress here only some general ideas on which it rests.

(i) A fundamental solution of the Markov process for the $A + B \rightarrow 0$ reaction under study can be presented in the form of an infinite set of coupled equations for the so-called *many-point-particle densities* $\rho_{m,m'}$.⁽⁷⁾ These many-point densities are averages over ensembles of *microscopic* densities $\hat{n}_v(\mathbf{r}, t)$ ($v = A, B$)

$$\rho_{m,m'} = \left\langle \prod_{i=1}^m \hat{n}_A(\mathbf{r}_i, t) \prod_{j=1}^{m'} \hat{n}_B(\mathbf{r}'_j, t) \right\rangle \quad (5)$$

where self-action singular terms are excluded. The derived set of kinetic equations for $\rho_{m,m'}$ ($m, m' = 0, 1, \dots, \infty$; $\rho_{0,0} = 1$) contains two kinds of contributions:

$$\frac{\partial \rho_{m,m'}}{\partial t} = \left. \frac{\partial \rho_{m,m'}}{\partial t} \right|_{\text{rec}} + \left. \frac{\partial \rho_{m,m'}}{\partial t} \right|_{\text{diff}} \quad (6)$$

due to reactant recombination and diffusion, respectively. For example, ^(7,16)

$$\begin{aligned} \left. \frac{\partial \rho_{m,m'}}{\partial t} \right|_{\text{rec}} = & - \sum_{i=1}^m \sum_{j=1}^{m'} \sigma(|\mathbf{r}_i - \mathbf{r}'_j|) \rho_{m,m'} \\ & - \sum_{i=1}^m \int \sigma(|\mathbf{r}_i - \mathbf{r}'_{m'+1}|) \rho_{m,m'+1} d\mathbf{r}'_{m'+1} \\ & - \sum_{j=1}^{m'} \int \sigma(|\mathbf{r}'_j - \mathbf{r}_{m+1}|) \rho_{m+1,m} d\mathbf{r}_{m+1} \end{aligned} \quad (7)$$

Here $\sigma(r)$ is the AB pair recombination rate. The first term in Eq. (7) describes all the possible ways in which m particles A can recombine with m' particles B, whereas the other terms describe the recombination of particles B with A (and vice versa) not belonging to a set of $(m+m')$ particles. In terms of the *black sphere* model (instant dissimilar particle recombination when their separation is less than some critical radius) we can write down

$$\sigma(r) = \sigma_0 \theta(r_0 - r), \quad \sigma_0 \rightarrow \infty \quad (8)$$

where $\theta(x)$ is the Heaviside step function. In the recombination model (8) characterized by the clear-cut recombination radius r_0 of a black, completely absorbing sphere the limiting transition of an instant recombination is assumed, $\sigma_0 \rightarrow \infty$. Use of Eq. (8) permits us to *simplify* maximally the kinetic equations of the diffusion-controlled reaction.

The diffusion contribution to the kinetic equations for the case of reactant interaction (drift in the field) reads⁽¹⁰⁾

$$\left. \frac{\partial \rho_{m,m'}}{\partial t} \right|_{\text{diff}} = - \sum_{i=1}^m \nabla_i \mathbf{J}_{m,m'}^{Ai} - \sum_{j=1}^{m'} \nabla_j \mathbf{J}_{m,m'}^{Bj} \quad (9)$$

where the *diffusion fluxes* are

$$\begin{aligned} \mathbf{J}_{m,m'}^{Ai} &= -D_A \left(\nabla_i \rho_{m,m'} + \frac{\rho_{m,m'}}{k_B T} \nabla_i W_{m,m'}^i \right) \\ \mathbf{J}_{m,m'}^{Bj} &= -D_B \left(\nabla_j \rho_{m,m'} + \frac{\rho_{m,m'}}{k_B T} \nabla_j W_{m,m'}^j \right) \end{aligned} \quad (10)$$

In two last equations the mean force potential $W_{m,m'}^i$ is introduced, for which

$$\begin{aligned}
\nabla_i W_{m,m'}^i &= \sum_{i' \neq i}^m \nabla_i U_{AA}(|\mathbf{r}_i - \mathbf{r}_{i'}|) + \sum_{j=1}^{m'} \nabla_i U_{AB}(|\mathbf{r}_i - \mathbf{r}'_j|) \\
&+ \int \frac{\rho_{m+1,m'}}{\rho_{m,m'}} \nabla_i U_{AA}(|\mathbf{r}_i - \mathbf{r}_{m+1}|) d\mathbf{r}_{m+1} \\
&+ \int \frac{\rho_{m,m'+1}}{\rho_{m,m'}} \nabla_i U_{AB}(|\mathbf{r}_i - \mathbf{r}'_{m'+1}|) d\mathbf{r}'_{m'+1} \quad (11)
\end{aligned}$$

where $U_{AA}(r)$, $U_{BB}(r)$, and $U_{AB}(r)$ are the pair potentials of particle interaction. The potential $W_{m,m'}^i$ is defined similarly. As is seen from Eq. (11), the mean force acting on a particle A has contributions from both direct interactions within a group of $(m + m')$ particles and indirect interactions (integral terms).

Single-point densities are nothing but macroscopic concentrations:

$$\rho_{0,0} = n_A(t), \quad \rho_{0,1} = n_B(t) \quad (12)$$

whereas the higher-order densities after extracting the concentration cofactors define a complete set of the *correlation functions*. They give us statistical information on the relative spatial distribution of reacting particles of both kinds, thus defining the *fluctuation spectrum* of the kinetics under study.

(ii) Similar to numerous solid-state problems leading to the infinite sets of equations (6) for the distribution functions, the $A + B \rightarrow 0$ bimolecular kinetics cannot be solved exactly and the relevant hierarchy of equations has to be decoupled, which shortens its fluctuation spectrum.

(iii) The use of a cutoff procedure for the reaction between charged particles has additional difficulties for the following reasons. Rigorous equations for the correlation functions contain both terms due to reaction itself and the drift in the field caused by the interaction potentials. As is well known from the statistical physics of Coulomb systems,⁽³⁾ in such problems the particle density cannot serve as a small parameter; as is shown in ref. 7, even for neutral particles, $L=0$, particle concentration decreases in time, but it enters the solution in the form of a product $n(t) \xi^3$ which *increases* in time. Similar to the physics of phase transitions and critical phenomena, the bimolecular reaction under study demonstrates spatial self-organization, and thus to decouple a set of the relevant kinetic equations, approximations widely used in the former theory could be effective.

(iv) As was shown in ref. 7, for neutral particles, $L=0$, practically the only useful approach is based on the Kirkwood superposition approximation⁽¹⁴⁾

$$\rho_{2,1} \Rightarrow \frac{\rho_{2,0}(\mathbf{r}_1, \mathbf{r}_2) \rho_{1,1}(\mathbf{r}_1, \mathbf{r}'_1) \rho_{1,1}(\mathbf{r}_2, \mathbf{r}'_1)}{\rho_{1,0}(\mathbf{r}_1) \rho_{1,0}(\mathbf{r}_2) \rho_{0,1}(\mathbf{r}'_1)} \quad (13)$$

Mathematical difficulties of the description of the fluctuation spectrum restrict the shortened hierarchy of equations at the level of the *joint correlation functions* for similar, $X_A(r, t)$ and $X_B(r, t)$, and dissimilar particles, $Y(r, t)$, describing correlations within pairs A–A, B–B, and A–B respectively:

$$\begin{aligned}\rho_{2,0} &= n_A^2(t) X_A(|\mathbf{r}_1 - \mathbf{r}_2|) \\ \rho_{0,2} &= n_B^2(t) X_A(|\mathbf{r}'_1 - \mathbf{r}'_2|) \\ \rho_{1,1} &= n_A(t) n_B(t) Y(|\mathbf{r}_1 - \mathbf{r}'_1|)\end{aligned}\quad (14)$$

The physical sense of these joint correlation functions is very transparent^(7,16): the average density of the v -type reactants at a distance r from the A-type reactant placed at the coordinate origin is

$$\begin{aligned}C_A(r, t) &= n_A(t) X_A(r, t), & v = A \\ C_B(r, t) &= n_B(t) Y(r, t), & v = B\end{aligned}\quad (15)$$

The joint correlation functions of similar (A–A, B–B) reactants characterize directly the fluctuations in a number of particles $v = A, B$ in an arbitrary volume V :

$$\frac{\langle (N_v - \langle N_v \rangle)^2 \rangle}{\langle N_v \rangle} = 1 + n_v(t) \int [X_v(r, t) - 1] dr \quad (16)$$

The second term of the rhs of Eq. (16) describes the deviation of the fluctuation spectrum from the Poisson spectrum (as it is seen on the joint density level). The only case when higher-order densities were used is in ref. 7 dealing with triple correlation functions in the $A + B \rightarrow B$ reaction.

(v) However, the Kirkwood approximation cannot be used for the modification of the drift terms in the kinetics equations, since it is too rough for Coulomb systems to give us the correct treatment of the charge screening.⁽³⁾ Therefore, the cutoff of the hierarchy of equations in these terms requires use of some *principally new approach*, keeping in mind that it should be consistent with the level at which the fluctuation spectrum is treated. In the case of the joint correlation functions we use here, this means that the only acceptable approach for us is the Debye–Hückel approximation.⁽³⁾ Let us consider it briefly. Put particle A at the origin. Keeping in mind the physical interpretation of the correlation function in Eq. (15), an expression $C_A(r, t) = n_A(t) X_A(r, t)$ defines the density of A's at the distance r from a given particle A at moment t . The charge density of these particles is

$$\hat{\rho}_A(r, t) = e_A C_A(r, t) = e_A n_A(t) X_A(r, t) \quad (17)$$

where e_A is a charge of particle A. The charge density of B's is

$$\hat{\rho}_B(r, t) = e_B C_B(r, t) = e_B n_B(t) Y(r, t) \quad (18)$$

The potential $\phi_A(r, t)$ produced by these charges in a medium with dielectric constant ε is obtained from the Poisson equation as

$$\nabla^2 \phi_A(r, t) = -\frac{4\pi}{\varepsilon} [\hat{\rho}_A(r, t) + \hat{\rho}_B(r, t)] \quad (19)$$

For equal concentrations $n_A(t) = n_B(t) = n(t)$ of particles with the Coulomb attraction, $e_A = -e_B$, the kinetic equations are simplified and will be written down below.

(vi) Therefore, the approximate treatment of the $A + B \rightarrow 0$ reaction for charged particles unavoidably requires a combination of several approximations: the Kirkwood superposition one for the reaction terms, Eq. (7), and Debye-Hückel for modification of the drift terms, Eq. (9), with self-consistent potentials. We do not discuss here the accuracy of the latter approximation, and note only that we found it to be correct enough for both qualitative and semiquantitative description of the charge screening.

The equation for the time development of macroscopic concentrations formally coincides with Eq. (1), but with a dimensionless reaction rate $K(t) \equiv K(t)/4\pi D r_0$ which is, generally speaking, *time dependent* and defined by the flux of the dissimilar particles via the recombination sphere of the radius r_0 . Using dimensionless units $n(t) \equiv 4\pi r_0^3 n(t)$, $r \equiv r/r_0$, and $t \equiv Dt/r_0^2$, we have, for the reaction rate usual for the black sphere, Eq. (8), for the flux over the recombination sphere

$$K(t) = \left. \frac{\partial Y(r, t)}{\partial r} \right|_{r=1} \quad (20)$$

The boundary condition imposed is the correlation weakening at infinity

$$\lim_{r \rightarrow \infty} Y(r, t), X_v(r, t) = 1 \quad (21)$$

and the recombination condition for dissimilar particles corresponding to the black-sphere model, $Y(r \leq 1, t) \equiv 0$, as well as the condition of zero flux through the origin for similar particles,⁽⁷⁾

$$\lim_{r \rightarrow 0} D_v r^2 \frac{\partial X_v(r, t)}{\partial r} = 0 \quad (22)$$

Equations (1) and (20) are coupled with the equation set for the joint correlation functions discussed above:

$$\frac{\partial Y(r, t)}{\partial t} = \nabla(\nabla Y(r, t) + Y(r, t) \nabla U(r, t)) - n(t) K(t) Y(r, t) \sum_{v=A, B} J[X_v] \quad (23)$$

$$\frac{\partial X_v(r, t)}{\partial t} = D_v \nabla(\nabla X_v(r, t) + X_v(r, t) \nabla U_v(r, t)) - 2n(t) K(t) X_v(r, t) J[Y] \quad (24)$$

Note that we use the dimensionless diffusion coefficients $D_A = 2\kappa$ and $D_B = 2(1 - \kappa)$, with $\kappa = D_A/(D_A + D_B)$, in Eq. (24).

When deriving the set of equations (23), (24) from a formally correct but infinite set of equations for the correlation functions of all orders, two principal approximations were used. The first one is *Kirkwood's superposition approximation*^(3,14) for three-particle densities leading to the appearance in Eqs. (23), (24) of the functionals

$$J[Z] = \frac{1}{2r} \int_{|r-1|}^{r+1} [Z(r', t) - 1] r' dr' \quad (25)$$

Its accuracy in the kinetic problems under study has been discussed^(7,15,16); it has been shown⁽¹⁶⁾ that the superposition approximation is quite correct for equal particle concentrations, $n_A = n_B$. In particular, the set (1), (20), (23), (24) applied to the reaction between neutral particles ($U = U_v = 0$) is able to reproduce the asymptotic decay laws found analytically in refs. 5 and 6 by means of other techniques.

Another approximation made is analogous to the Debye-Hückel one⁽³⁾ and permits us to express the self-consistent potentials via particle concentrations and the joint correlation functions⁽¹⁰⁾

$$\nabla^2 U_v(r, t) = -n(t) L[X_v(r, t) - Y(r, t)], \quad \lim_{r \rightarrow 0} r U_v(r, t) = L \quad (26)$$

where $U(r, t) = -\frac{1}{2}[U_A(r, t) + U_B(r, t)]$ (dimensionless units are used).

To demonstrate the importance of charge screening in a many-particle system, it should be mentioned that the substitution of potentials U_v entering Eqs. (23), (24) by nonscreened potentials $U_v = L/r$ leads to the *Coulomb catastrophe*, manifested by the unlimited increase of the reaction rate $K(t)$.⁽¹⁰⁾

If particles have different diffusion coefficients, $D_A \neq D_B$, their correlation functions no longer coincide, $X_A \neq X_B$, which results also in different screening effects for these two kinds of particles—see Eq. (26).

Unlike the case of the neutral reactants, where the analytical solution reveals the auto-model behavior in coordinate r/ξ , in our case of charged

particles the singular solutions arise on the spatial scale of the order of the recombination radius r_0 , thus precluding such a simplified analytical analysis. Therefore, we will compare the semiquantitative estimates presented in Section 1 with numerical calculations of our kinetic equations.

3. RESULTS

A solution of the kinetic equations with singular (e.g., Coulomb) potentials is a nontrivial problem. The efficient calculation of Eqs. (23), (24) needs to use difference schemes whose coefficients depend on potentials. Since these potentials $U_v(r, t)$ in their turn depend on the correlation functions [see Eq. (26)], we have to handle nonlinear equations, for which the iterative procedure developed in ref. 10 is used.

The asymptotic ($t \rightarrow \infty$) treatment of the set of nonlinear integro-differential equations is quite difficult even as a computational problem, since solution stability requires the use of small time increments in a mesh, and thus we could reach $t = 10^5$ only (in dimensionless units). Besides, in the particular case of asymmetric mobility, $D_A = 0$, we observe a spatial particle distribution revealing strongly developed singular properties, which requires the additional reduction of the coordinate increment.

Figure 1 shows the time development of particle concentrations. At long times the kinetics for symmetric ($D_A = D_B$) and asymmetric ($D_A = 0$) cases differ significantly: in the latter case the reaction proceeds more

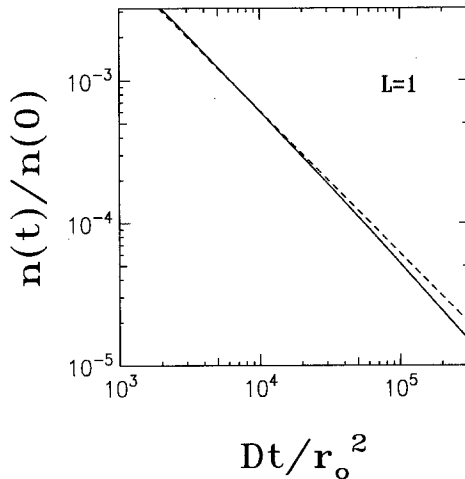


Fig. 1. Particle concentration $n(t)$ as a function of time. Full curve, $D_A = 0$; dashed curve, $D_A = D_B$. Parameters are $L = 1$, $n(0) = 0.1$.

quickly. Note that the choice of the parameter $L=1$ corresponds to the weak electrostatic field; the Onsager radius R is small and coincides with the recombination sphere radius r_0 . The initial dimensionless concentration $n(0)=0.1$ is also not too large: it is only 10% of the maximum concentration which could be achieved under irradiation.⁽¹⁶⁾ The magnitudes of these two parameters were chosen to save time in our computations.

The difference in the kinetics for two limiting cases $D_A=0$ and $D_A=D_B$ becomes more obvious in terms of the *current critical exponents* defined as

$$\alpha(t) = -\frac{d \ln n(t)}{d \ln t} \quad (27)$$

It yields the *slope* of decay curves shown in Fig. 1. The conclusion can be drawn from Fig. 2 that in the symmetric case we indeed observe well-known algebraic decay kinetics with $\alpha(\infty)=1$ corresponding to a time-independent reaction rate, Eq. (1). However, in the asymmetric case the critical exponent increases in time, thus indicating the peculiarity of the kinetics as we qualitatively estimated in Section 1.

The dimensionless reaction rate $K(t)$ as a function of time for different values of $\kappa = D_A/D$ is plotted in Fig. 3. One can see again that as $t \rightarrow \infty$, in the symmetric case it indeed reaches the steady-state value described by Eqs. (2)–(4). However, in the asymmetric case there is *no* steady state: it is seen very well from the additional curve for $D_A/D = 0.01$ —here the kinetics

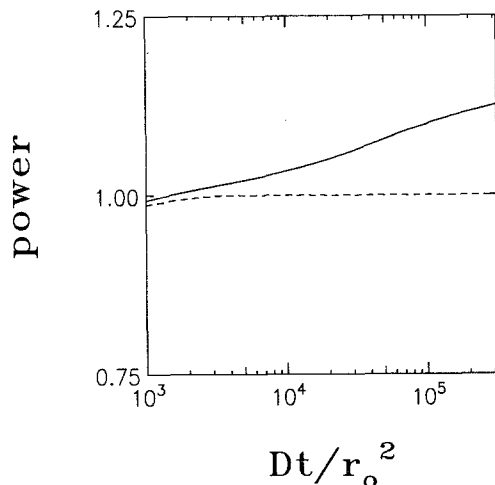


Fig. 2. The critical exponent, Eq. (27), as a function of time. Parameters and key as in Fig. 1.

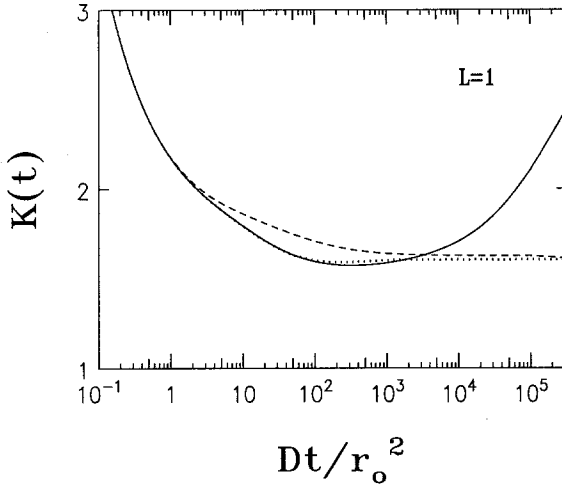


Fig. 3. The time development of the reaction rate $K(t)$. Dashed curve, symmetric case ($D_A = D_B$); solid curve, asymmetric case ($D_A = 0$); dotted curve, $D_A/D = 0.01$.

is the same as for the asymmetric case up to $Dt/r_0^2 \leq 10^3$, but at greater times it follows the kinetics known for the symmetric situation.

An unusual behavior of the reaction rate is clarified in Fig. 4: the screening factor $S(r, t)$ shown here is obviously *nonequilibrium*; its asymptotic value $S_0(t)$ increases in time. [As was said above, at low

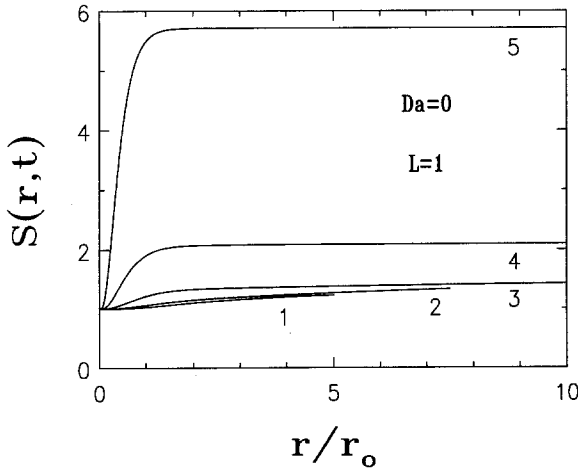


Fig. 4. The screening factor in the asymmetric case. Parameters as in Fig. 1. Curves 1-5 correspond to the dimensionless time Dt/r_0^2 : $10^1, 10^2, 10^3, 10^4$, and 10^5 , respectively.

concentrations the values of $S_0(t)$ correspond to the mean number of particles A in their aggregates existing on the background of a uniform B distribution.] Note that, as noted in Section 1, this aggregation has purely statistical character.

For the asymmetric case the spatial distribution of A particles reveals quite singular behavior (“raisins in dough”) (Fig. 5). The joint correlation function for similar particles, $X_A(r, t)$, has a sharp maximum near the coordinate origin: its amplitude increases monotonically with time, but it decreases by several orders of magnitude as r increases from zero up to several times r_0 . Correspondingly, the screening factor shown in Fig. 4 approaches, at the same distance, to its asymptotic value. The physical meaning of $X_A(r, t)$ is just a ratio of the probability density to find some A particle at a final distance r from a given A to that at their random distribution ($r \rightarrow \infty$). Hence, the power-law increase in $X_A(r, t)$ maximum with time seen in Fig. 5 indicates clearly *strong aggregation* of immobile A particles.

Joint distribution of B–B and A–B pairs is shown in Fig. 6. The distribution of similar mobile particles B at long times in the asymmetric case practically is the same as in the symmetric case (when $X_A = X_B$). The behavior of $X_B(r, t)$ is determined by the Coulomb repulsion of B’s for which the nonequilibrium screening effect does not take place. In its turn, some deviation for the joint dissimilar functions $Y(r, t)$ seen in Fig. 6 for the symmetric and asymmetric cases is a direct consequence of different

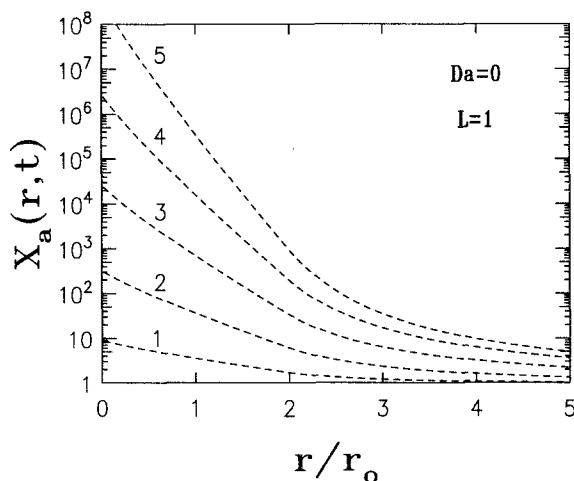


Fig. 5. The joint correlation function X_A of similar particles A in the asymmetric case. Key as in Fig. 4.

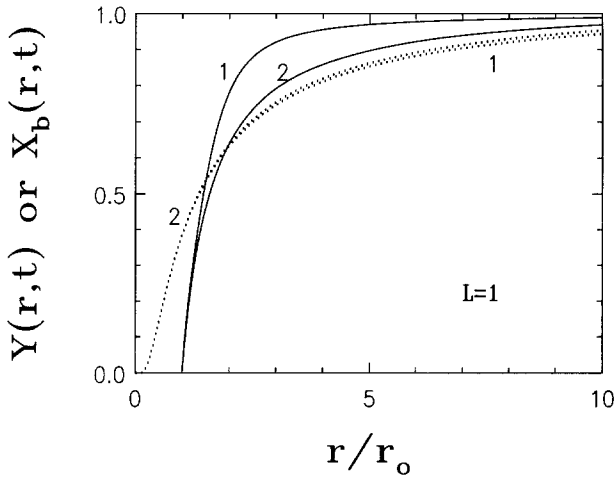


Fig. 6. The joint correlation function of dissimilar particles [$Y(r, t)$, solid curve] and that of similar particles [$X_b(r, t)$, dashed curve]. Parameters are $L=1$, $n(0)=0.1$. (1) Asymmetric case; (2) symmetric case.

screening effects: in the latter case the effective recombination radius increases in time, which results in an increase of the $Y(r, t)$ gradient at $r=r_0$ [see Eq. (20)]; at long times this correlation function itself approaches the Heaviside steplike form.

Lastly, Fig. 7 demonstrates the *intermediate case* of slowly, mobile A

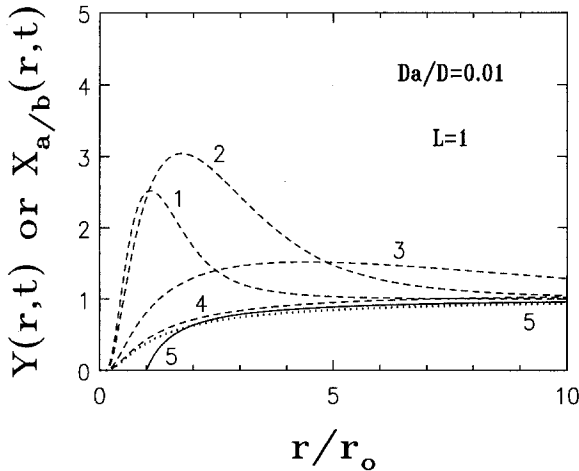


Fig. 7. The joint correlation functions in the intermediate case, $D_A/D=0.01$. Solid curve, $Y(r, t)$; dashed curve, $X_A(r, t)$; dotted curve, $X_B(r, t)$.

particles. It is seen very well that now aggregates of A are dissolved by diffusive motion and their distribution is no longer singular. At long times the difference between correlation function X_A and X_B becomes negligible.

The screening parameter $S(r, t)$ for the symmetric case, $D_A = D_B$, is shown in Fig. 8. It demonstrates clearly the formation of a quasi-equilibrium charge screening; at any time, $S(r, t) \leq 0$ and its asymptotic value $S_0(t)$ decays monotonically in time.

The nonequilibrium particle distribution is clearly observed through the joint correlation functions plotted in Fig. 9. Note that under the linear approximation^(1,2) the correlation function for the dissimilar defects $Y(r, t)$ increases *monotonically* with r from zero to the asymptotic value of unity; $Y(r \rightarrow \infty, t) = 1$. In contrast, curve 1 in Fig. 9 ($t = 10^1$) demonstrates a *maximum* which could be interpreted as an enriched concentration of dissimilar pairs, AB, near the boundary of the recombination sphere, $r \geq r_0$. With increasing time this maximum disappears and $Y(r, t)$ assumes the usual smoothed-step form. The calculations show that such a maximum in $Y(r, t)$ takes place within a wide range of initial defect concentrations and for a random initial distribution of both similar and dissimilar particles used in our calculations: $X_v(r, 0) = Y(r > 1, 0) = 1$. Mutual Coulomb repulsion of similar particles results in a rapid disappearance of close A-A (B-B) pairs separated by a distance $r < L$ [seen in Fig. 9 as a decay of $X_v(r, t)$ at short r with time]. On the other hand, it stimulates strongly the mutual approach (aggregation) of *dissimilar* particles leading to the maximum for $Y(r, t)$ at intermediate distances observed in Fig. 9.

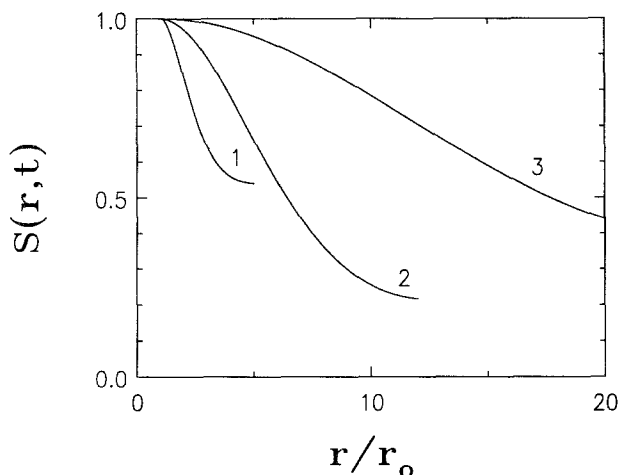


Fig. 8. The screening parameter in the symmetric case, $D_A = D_B$. Parameters are $n(0) = 1$, $L = 5$. Curves 1-3 correspond to the dimensionless time $Dt/r_0^2 = 1, 10^1, 10^2$, respectively.

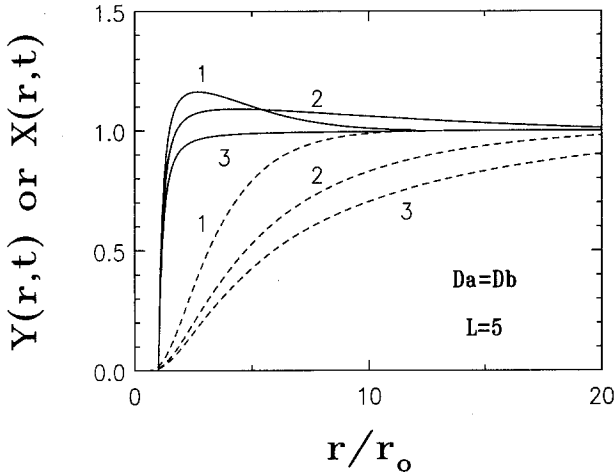


Fig. 9. The joint correlation functions for the case $D_A = D_B$. Solid curves, dissimilar defects, $Y(r, t)$; dashed curves, similar defects, $X_A(r, t) = X_B(r, t)$. Parameters $n(0) = 1$, $L = 5$. Curves 1–3 correspond to the dimensionless time equal to 10^1 , 10^2 , 10^5 , respectively.

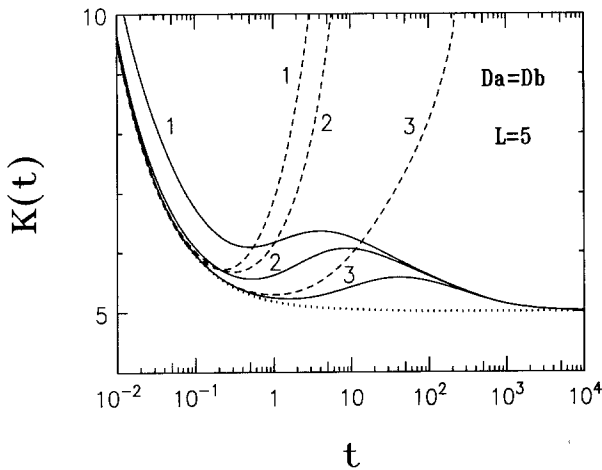


Fig. 10. The role of nonequilibrium charge screening in eliminating the Coulomb catastrophe: the dimensionless reaction rate vs. time. Dotted curve, the Debye theory^(1,2) (no screening and similar particle correlation); dashed curves, the solution of the kinetic equations incorporating these correlations but neglecting screening; solid curves, screening is taken into account. Parameters $L = 5$, $D_A = D_B$. Curves 1–3 correspond to dimensionless time 10^1 , 10^2 , 10^5 , respectively.

In its turn, as follows from Eq. (20), the nonmonotonic behavior of $Y(r, t)$ results in a similar behavior of the reaction rate $K(t)$ in time (Fig. 10). The local maximum of $K(t)$ observed at $t = 10^1$ (for a given L) for different initial concentrations likely arises due to the initial conditions used, which do not take into account peculiarities of the spatial distribution of charged particles: a more adequate one would be a quasiequilibrium pair distribution with incorporated potential screening.

The role of the nonequilibrium charge screening is emphasized by calculations neglecting such a screening, i.e., when Eqs. (26) are omitted and $U_v = L/r$ is postulated. In this case mutual repulsion of similar particles accompanied by the attraction between dissimilar particles are characterized by the *infinite* interaction radius between particles, which leads immediately to the *Coulomb catastrophe*—an infinite increase in $K(t)$ in time shown in Fig. 9. This effect is independent of the choice of the initial defect distributions for both similar and dissimilar particles. On the other hand, an incorporation of Coulomb screening makes Eqs. (2)–(4) asymptotically valid for any initial distribution of particles.

4. CONCLUSION

In the present paper a novel formalism of the many-point particle densities is applied to study many-particle effects and charge screening in the kinetics of bimolecular reactions $A + B \rightarrow 0$ with Coulomb interaction between reactants. It is demonstrated that this screening, unlike standard Debye–Hückel theory, has essentially nonequilibrium character. For equal reactant mobilities (the so-called symmetric case) neglect of this fact leads to the Coulomb catastrophe (an infinite increase of the reaction rate in time), whereas its proper incorporation into kinetic equations results in both the moderate increase of the reaction rate at intermediate times and nonmonotonic behavior of the joint correlation functions of dissimilar reactants.

In the asymmetric case ($D_A = 0$) similar immobile particles A become aggregated in the course of reaction and, as $t \rightarrow \infty$, the relevant reaction rate no longer has a steady state, but increases in time, leading to accelerated particle recombination. We hope that the theory developed in the present paper could be useful for interpreting experimental data on processes in such dense Coulomb systems as plasmas, ionic solids and liquids, and electrolyte solutions.

ACKNOWLEDGMENTS

We are greatly indebted to Prof. A. Blumen and Dr. H. Schnörer for numerous stimulating discussions and warm hospitality during our visits to Bayreuth University. V.K. also gratefully acknowledges the support from the Alexander von Humboldt Foundation.

REFERENCES

1. H. Eyring, S. H. Lin, and S. M. Lin, *Basic Chemical Kinetics* (Wiley, New York, 1980).
2. P. Debye, *J. Electrochem. Soc.* **32**:265 (1942).
3. R. Balescu, *Equilibrium and Non-Equilibrium Statistical Mechanics* (Wiley, New York, 1975).
4. A. B. Doktorov, A. A. Kipriyanov, and A. I. Burshtein, *Sov. Opt. Spectr.* **45**:497 (1978).
5. A. A. Ovchinnikov and Ya. B. Zeldovich, *Chem. Phys.* **28**:215 (1978).
6. D. Toussaint and F. Wilczek, *J. Chem. Phys.* **78**:2642 (1983).
7. V. N. Kuzovkov and E. A. Kotomin, *Rep. Progr. Phys.* **51**:1479 (1988).
8. Special issue of *J. Stat. Phys.* **65**:(5/6) (1991).
9. B. J. West, R. Kopelman, and K. Lindenberg, *J. Stat. Phys.* **56**:1429 (1989).
10. V. N. Kuzovkov and E. A. Kotomin, *Chem. Phys.* **98**:351 (1985).
11. A. G. Vitukhnovsky, B. L. Pyttel, and I. M. Sokolov, *Phys. Lett. A* **128**:161 (1988).
12. N. Itoh, *Adv. Phys.* **31**:49 (1982).
13. M. N. Kabler, In *Point Defects in Solids*, Vol. 1, J. Crawford, ed. (Plenum Press, New York, 1972), Chapter 4.
14. J. G. Kirkwood, *J. Chem. Phys.* **76**:479 (1935).
15. H. Schnörer, Ph.D. thesis, Universität Bayreuth (1991).
16. V. N. Kuzovkov and E. A. Kotomin, *Rep. Progr. Phys.* **55**:2079 (1992).